Environment Canada | Environnement Canada

Atmospheric Environment Service | Service de l'environnement atmosphérique

HYDROMETEOROLOGY AND MARINE DIVISION

CANADIAN CLIMATE CENTRE

DIVISION DE L'HYDROMETEOROLOGIE ET CLIMATOLOGIE MARITIME

CENTRE CLIMATOLOGIQUE CANADIEN

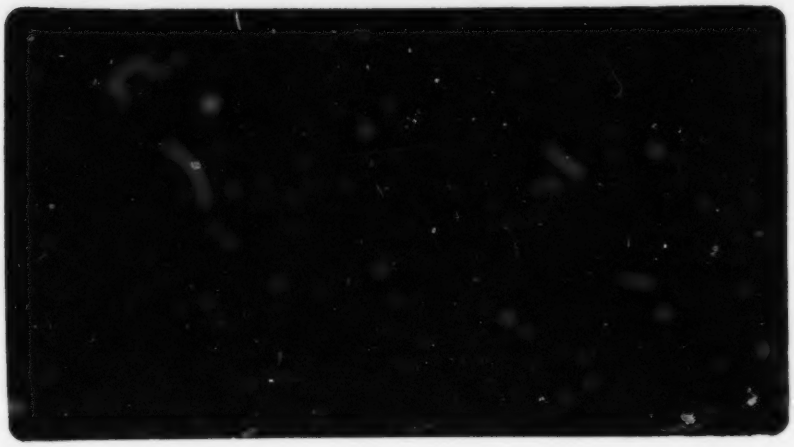

ATMOSPHERIC ENVIRONMENT SERVICE
4905 DUFFERIN STREET
DOWNSVIEW, ONTARIO
M3H 5T4

SERVICE DE L'ENVIRONNEMENT ATMOSPHERIQUE
4905 DUFFERIN STREET
DOWNSVIEW, ONTARIO
M3H 5T4

Canada

91-04378/

IMPLEMENTATION OF AN ALGORITHM TO ESTIMATE REGIONAL EVAPOTRANSPIRATION USING SATELLITE DATA

N. Bussières and P.Y.T. Louie

June 1989

Hydrometeorology and Marine Divison
Canadian Cimate Centre

Atmospheric Environment Service
4905 Dufferin Street
Downsview, Ontario M3H 5T4

SUMMARY

This report describes the implementation of a simple scheme to estimate evapotranspiration from satellite radiance measurements, in cloud free situations. Although the primary objective was to estimate the evapotranspiration field, the methodology also required the derivation of several intermediate fields which included albedo, surface temperature and net radiation. These intermediate fields have great value in various applications. The scheme uses visible and infrared channels from GOES, plus air temperature and upper air soundings of temperature and moisture. Data requirements and processing are discussed in detail. Validation and error assessment of intermediate data fields are made.

RÉSUMÉ

Ce rapport décrit, pour des situations sans nuages, l'implantation d'une méthode simple pour l'estimation de l'évapotranspiration à partir des radiances mesurées par satellite. Bien que l'objectif principal est de faire l'estimation du champ d'évapotranspiration, la méthode nécessitait la génération de plusieurs champs intermédiaires, incluant l'albédo, la température de surface et le bilan du rayonnement. La valeur de ces champs intermédiaires est très utile dans nombre d'applications. Cette méthode utilise les données visible et infrarouge du satellites GOES, ainsi que la température de l'air et des sondages en altitude de température et d'humidité. Les détails du traitement de données sont discutés. On vérifie la validité les champs intermédiaires et on évalue les erreurs associées à ces champs.

PREFACE

A feasibility study on estimating evapotranspiration using satellite data appeared as CCC Report No. 87-12. Since then, the authors undertook software implementation, following the procedures outlined in that report. This implementation effort revealed difficulties with interpretation of the text of chapter three. This was due to missing symbols in a few equations and specially in the formulation of equations (9) and (10). For this reason and also to incorporate corrections suggested by readers on the scientific content and style, sections of CCC Report No. 87-12 were rewritten and included in this current document.

TABLE OF CONTENTS

Page

Summary i

Resumé i

Preface ii

Table of Contents iii

List of Tables iii

List of Figures iv

Acknowledgements v

1. Introduction 1

2. Implementation of the Residual Energy Budget Method 2

2.1 Description of the Method 2

2.2 Implementation 5

3. Validation and Error Estimates 11

References 16

Appendix 1: Additional Information 25

LIST OF TABLES

Table		Page
1	Surface classification for gridded inventory	10
2	Relative Contribution of Net Radiation and Heat Flux to ET Estimates	14

LIST OF FIGURES

Figure		Page
1	Relationship between lysimeter ET and net radiation	3
2	Data flow diagram for implementation of the ET algorithm	7
3	GOES infrared on July 24, 1985, at 1800 UCT	19
4	GOES visible picture on July 24, 1985, at 1800 UCT	19
5	July 24, 1985, 1800 UCT cloud mask based on level 22 of GOES VIS data	20
6	1800 UCT estimated albedo for GOES view point	20
7	Surface temperatures (^{O}C) estimated from GOES IR channel	21
8	Air temperature (objective analysis of land stations)	21
9	Predominant land classification	22
10	24-hour net radiation estimated from satellite for July 24, 1985	22
11	Heat Transfer Term for July 24, 1985	23
12	24-hour evapotranspiration estimated from satellite on July 24, 1985	23
13	Lake Erie Surface Water Temperature Analysis, 0800 UCT, July 23, 1985	26
14	Lake Ontario Surface Water Temperature Analysis	26

ACKNOWLEDGEMENTS

We wish to thank personel of the Hydrometorological Services Section of the Canadian Climate Centre for their courtesy in providing access and assistance to the mini-computer based CLI-GRID system. Thanks are also extended to J.G. Irbe for assistance with the temperature correction algorithm and for the provision of satellite water temperature estimates. Finally, we wish to thank K. Czaja for assistance in preparing the Figures.

INTRODUCTION

Evapotranspiration (ET) is an important process in many climatological applications. In agriculture, hydrology and climate modelling, it is a key component of the water and energy budgets. Direct ET measurements are difficult to make and at best provide only point values. Presently, regional values of ET must be estimated by models using standard meteorological network data as input. Remotely sensed data from meteorological satellites have the potential for improving regional estimates of ET. Recognizing this potential, many researchers have worked on developing ET models that accept remotely sensed measurements as input variables.

Bussières and Loule (1987) conducted a study to determine the feasibility of producing operational ET estimates on the regional scale. The study classified satellite data techniques into two groups: a) iterative energy-balance model inversion (Taconet et al 1986) and b) residual energy budget (Jackson et al 1977).

Method (a) uses an energy balance model to estimate the surface temperature. Iterations are made until the estimated temperature compares, within pre-determined limits, to a temperature value estimated from remotely sensed data. At this point, the model is inverted, giving the fluxes. This method may provide an excellent representation of reality but its use is currently limited to case studies.

Method (b) is simpler and is considered more suitable for operational use; the latent heat flux is computed as a residual of the energy budget equation formulated to use remotely sensed data. In the following, this method is applied to daily estimates of ET, under non-cloudy conditions. Chapter two describes the method and its implementation in a multi-data set environment. Chapter three describes validation of the generated fields and points out some unresolved problems.

2. IMPLEMENTATION OF THE RESIDUAL ENERGY BUDGET METHOD

The rate of ET is controlled by temperature, humidity, net radiation and wind. It depends also on the availability of water at or below the surface, the nature of the surface and the physiological state of the vegetation.

2.1 Description of the method

Termed "residual energy budget" by Rambal et al (1985), the method was introduced by Jackson et al (1977). Their concept was to use remotely sensed temperature in the evaluation of the expression:

$$LE^{24} \approx R_n^{24} - B\,(T_s - T_a)^i \qquad (1)$$

$$B \approx (R_n^{24} / R_n^i)\ \overline{\rho\, c_p / r^i_{ah}} \qquad (2)$$

where:

LE^{24} = 24 hour total ET

R_n^{24} = 24 hour net radiation

$(T_s - T_a)^i$ = instantaneous canopy to air temperature difference near midday

R_n^i = instantaneous net radiation around midday

r^i_{ah} = turbulent diffusion resistance to heat transport (a function of wind velocity, atmospheric stability and surface roughness)

ρ = air density

c_p = specific heat of air

Equation 1 represents the energy budget, for a duration of 24 hours, and with the ground heat component neglected. Peculiar, however, is the heat flux term. It uses temperature measurements made at a point in time to produce a heat flux valid for the duration of a day. Time scale conversion is thus handled as shown in Equation 2. Selection of midday for the time of measurement corresponds often to the time of maximum heat flux.

Daily lysimeter data and net radiation comparisons for grassland, by Kotoda et al (1985), are plotted in Figure 1 and display a linear relationship. This is an example of the role of the net radiation term in Equation 1. In that example, the temperature term would be a second order correction to the estimate of ET from net radiation.

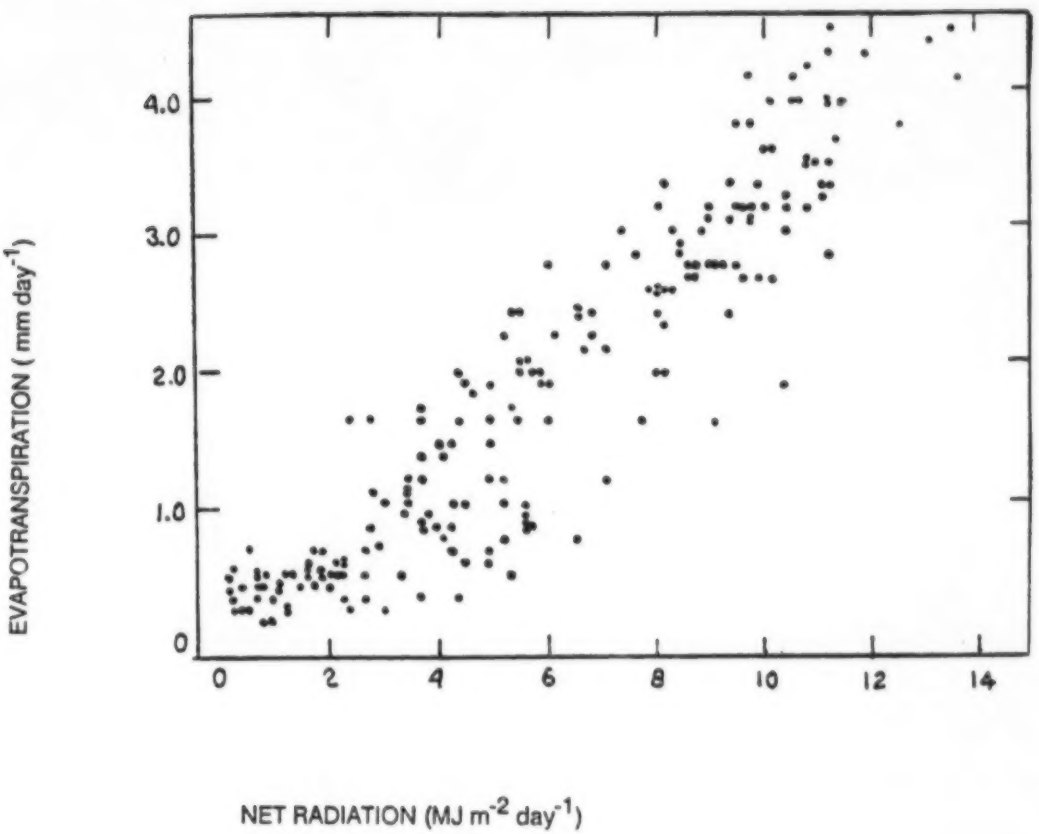

Figure 1. Relationship between lysimeter evapotranspiration and net radiation, over grass, in 1982. From Kotoda et al (1985).

Seguin and Itier (1983) estimated errors of the method below 10 and 20 percent for monthly sums of their ET outputs. The reader is directed to their work for an excellent discussion on the physical aspects of the method. As in Jackson et al (1977), the same authors suggested some values for the "B" coefficient. Rambal et al (1985) also illustrated how to model the values of "B" for 4 types of vegetation from data on 4 different days.

Because of limitations in the modeled estimates of the B term, due for example to neglecting the effect of wind and soil moisture, large errors in individual estimates of ET can be expected in a number of cases. Improvement of the data base and better calibration efforts would certainly help to overcome this classical problem.

The "B" coefficient involves the aerodynamic and surface resistances which are well known (Serafini 1987) sources of uncertainty. Nieuwenhuis et al (1986) discussed the limitations of the "B" term. It must be tuned according to the climate and the surface with clear days being essential for applying the method. The same authors suggested the following alternative form:

$$LE^{24} \approx LE_p^{24} - B' (T_c - T_c^*) \quad (3)$$

where:

B' = calibration constant

T_c^* = temperature of the crop that is potentially transpiring under optimal soil moisture condition

T_c = temperature of the crop under the restriction of soil moisture condition

LE_p^{24} = 24 hour potential ET flux (see for example Monteith 1973)

T_c^* and T_c are estimated from thermal IR data. Areas known to be adequately supplied with water (possibly low elevation areas) would be selected for the estimation of T_c^*. Equation 3 states the reduction in ET based on the difference in crop temperatures. The authors of this technique presented heat images showing the variability of temperature with vegetation in connection with computed maps of the deficit in ET. They concluded that this type of analysis over cultivated land is valid only with remote sensing from aircraft, which has the necessary resolution. Remote sensing by satellite provides adequate time coverage but its spatial resolution is inadequate for the size of cultivated plots. Because of the necessity of determining the difference between T_c^* and T_c, this seems indeed to be a limitation for using the method of Nieuwenhuis et al (1985) with satellite data.

Reiniger and Seguin (1986) provided an intercomparison of the iterative energy balance model inversion (TERGRA, TELL-US, TELOP and SEAL models) and the residual energy budget methods. They concluded that all methods must be used in parallel with ground truth since they are more suited for delineating relative changes in ET patterns than absolute values.

The same authors approved the use of Equation 1 as an alternative solution to complex modeling. They also concluded that the use of the consecutive night/day temperature difference (suggested by Price, 1980) would not improve ET estimates. Price (1980) used the difference between maximum and minimum temperature as an approximation for the derivative of the temperature relative to time, to compute the transfer of energy through the ground. This term of the energy balance is neglected in the derivation of Equation 1.

2.2 Implementation

Our example for an implementation strategy uses the equations and values given in Rambal et al (1985):

$$LE^{24} \approx R_n^{24} - B\,(T_s - T_a)^{3/2} \qquad \text{for } T_s > T_a \qquad (4)$$

This is the unstable case, and B, expressed in mm /^{o}C - day, is given as: 0.32 for shrubland, 0.43 for open woodland, 0.68 for mid-dense woodland. For dense woodland, the value of B is 2.4, which, according to Rambal et al, is probably an overestimate. More values can be found in the literature.

Stable conditions (Ts < Ta) are likely to occur only under advective conditions at midday. In their study of the stable case, Seguin and Itier (1983) suggested the use of the Jackson et al (1977) equation, with B values smaller than in the unstable case:

$$LE^{24} \approx R_n^{24} - B\,(T_s - T_a) \qquad \text{for } T_s < T_a \qquad (5)$$

Uncertainty in Equations 4 and 5 depends on the uncertainty in the temperature difference, the B coefficient and the net radiation estimate. In a case study, Cooper et al (1984) determined uncertainty values of $(T_s - T_a)$, to be about $\pm$ 3.8 ^{o}C. In our evaluation, if B is 0.32 (for shrubland), the corresponding uncertainty due to temperature in the B(Ts - Ta) term is $\pm$ 1.2 mm/day. In energy terms, with the latent heat of evaporation of water being (2.45 x 10^{6}) Joule/Kg, the corresponding uncertainty is:

$$U = \pm\, 1.2 \times 10^{-3}\ \frac{m}{day} \times 2.45 \times 10^{6}\ \frac{Joule}{Kg} \times 1000\ \frac{Kg}{m^3}$$

$$U = \pm\, 2.9\ MJ / day\ m^2$$

This is rather significant compared to the incoming solar daily radiation range of 17.5 to 28.5 MJ m^{-2} reported for the cases studied by Rambal et al. Absolute values of ET can be obtained but the merit of the results will lie more in delineating the areal variation in ET.

For test implementation of the technique, an environment that accepted both remotely sensed and objectively analyzed conventional data was required. The CLI-GRID system (Hogg et al 1986) was used. CLI-GRID allows the production of various independent gridded fields that could be combined to give an ET map. CLI-GRID mesh size is about 4 km.

In order for the reader to better judge the level of effort required, it is convenient to consider the implementation of methodologies for building each field and data set as separate modules. Contrary to the iterative model inversion method, the residual energy budget method does not suppose an implicitly balanced equation set. Since more input variables are used than in modeling, more errors are possible. This imposes a need for verification of intermediate steps (point comparisons and allowance for possible ranges). The existence of intermediate data sets is on the other hand particularly useful. Albedo, surface temperature and net radiation data fields have great value in various applications. The following implementation scenario is tailored to facilitate the examination of intermediate data.

A) Data flow diagram

Figure 2 (next page) illustrates the relationship between the data sets required. Squares represent co-located gridded arrays (256 x 128 elements in CLI-GRID). Disk volume symbols represent ungridded data sets. Processes applied to data sets are indicated in plain language between the various surfaces. Building of arrays and testing proceeds from top of the diagram towards the bottom right. Arrows indicate the directions of the data flow. Satellite data are used extensively.

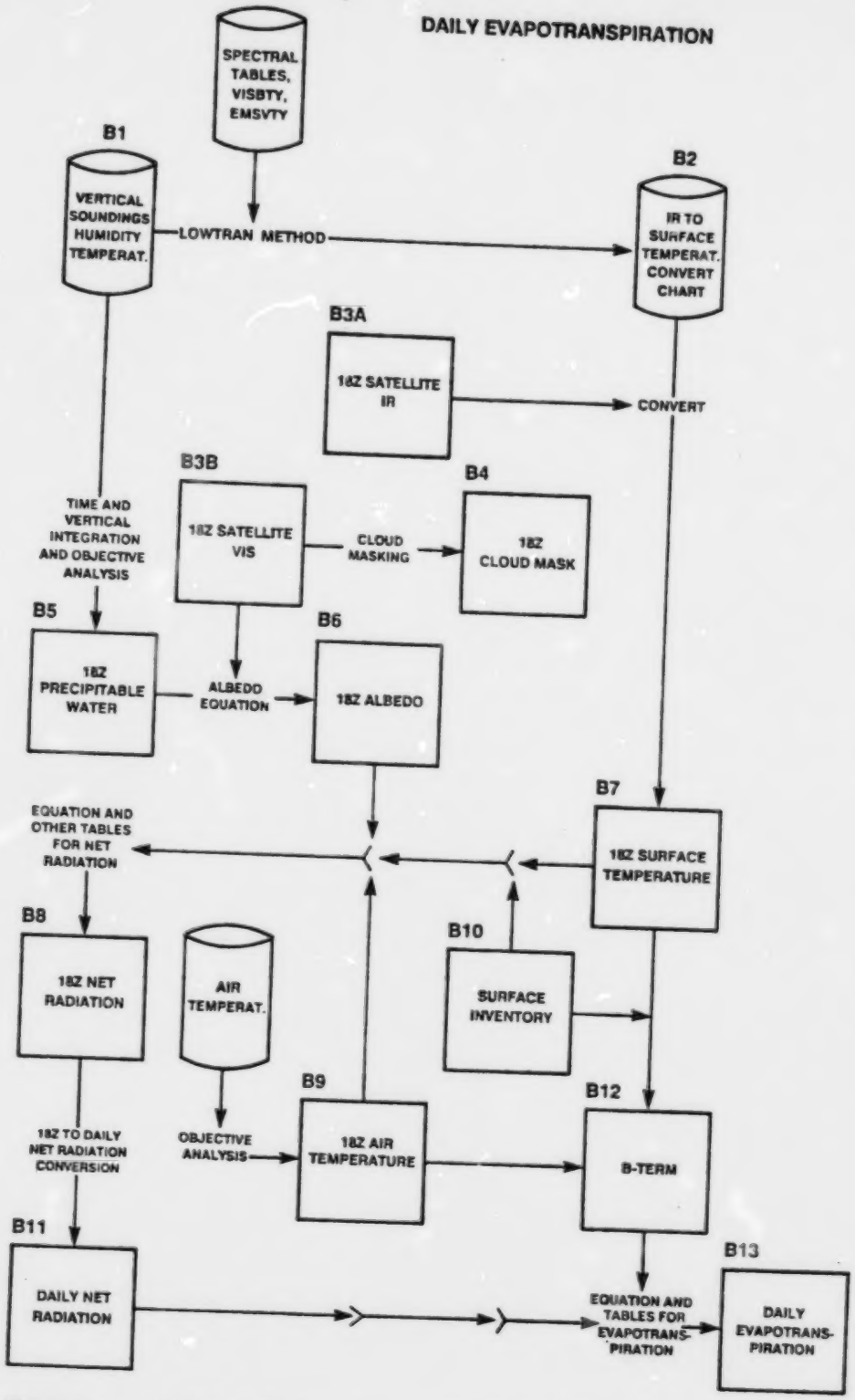

Figure 2. Data Flow Diagram for implementation of ET algorithm

B) Data sets

B.1 Vertical soundings of the atmospheric temperature and water content.

These are needed for the vertical integration of water content. Precipitable water content is later used to create data set B6.

B.2 IR to surface temperature conversion table

This table implements satellite count to radiance conversion. It also contains atmospheric corrections computed with the LOWTRAN module (see irbe et al, 1982).

B.3 1800 UCT satellite infrared and visible digital counts.

The infrared data should come from NOAA Polar orbiter satellites, for which most of the work was done for atmospheric corrections and for the evapotranspiration method. To be consistent, the visible data should come from the same satellite, but there is no problem using GOES data to create the cloud mask data field.

B.4 Cloud mask

GOES data has a resolution of about 2 km (VIS) and 8 km (IR) GOES. According to Tsonis (1983), clear daytime conditions occur when the GOES VIS count, normalized for the solar zenith angle, is below 23. Under these conditions, the VIS sensors respond mostly to solar radiation reflected by the surface. Under cloudy areas, ET is not available with this method and all processing requiring satellite data is skipped for grid locations classified as cloudy.

B.5 An objective analysis of the precipitable water content (u).

Precipitable water content values computed at sounding locations, for the purpose of correcting visible and infrared data, can be used also in more data processing related to net radiation estimates. It is useful to obtain these values on a regular grid. Interpolation by weights computed on the inverse square of the distance suffice, given the low density of upper air stations.

B.6 Albedo map

It is deduced from GOES VIS maps and is strictly valid from the satellite point. Clear sky albedo is proportional to the observed radiance from a pixel. Benchimol and Hay (1986) quote the following expression:

$$A \approx \frac{(K\uparrow - K_0 \alpha)}{S\ [1 - a(u_2)]\ (1 - \alpha_1)} \qquad (5)$$

with:

$$S = Ko\ (1 - \alpha)\ (1 - a(u_1)) \qquad (7)$$

where:

$K\uparrow$ = radiance monitored by the satellite
K_o = extraterrestrial irradiance a function of the latitude, solar declination angle and time of day
S = solar radiation incident at the surface
$a(u_1)$ = water vapor absorption coefficient for solar zenith angle
$a(u_2)$ = water vapor absorption coefficient for satellite viewing angle
α, α_1 = Rayleigh scattering coefficients for direct and diffuse radiations
u_1, u_2 = precipitable water content along the path

Detailed guidelines for correctly evaluating these expressions are given in their paper and in Chapter 3 of Benchimol (1985). The value of $K\uparrow$ must be properly determined and corrected from the satellite radiance calibration to relate to the digital count given by its sensor. An albedo map provides a convenient intermediate step for data verification.

B.7 Midday Surface temperatures estimated from satellite IR

Navigated NOAA IR data are converted to temperatures through the application of a previously created table.

B.8 Instantaneous net radiation fields (Rn^i).

These are estimated from satellite data sources. Approximately:

$$R_n^i \approx (1 - A)\, S + R\downarrow - e_{sfc}\, \sigma\, T_s^4 \qquad (8)$$

where:

e_{sfc} = IR emissivity of the surface
σ = Stefan-Boltzmann constant

Tabulated values of emissivity of various surfaces are available in the literature. The albedo (Equation 6) might be replaced directly in (8). The $R\downarrow$ term can be evaluated approximately with Brunt's empirical formula:

$$R\downarrow = e_{air}\, \sigma\, T^4_{air}\, (.61 + .05\, (v)^{1/2}) \qquad (9)$$

where:

v = vapor pressure (mm Hg)
e_{air} = IR emissivity of air

B.9 Objective analysis of midday air temperatures (T_a) from reporting stations.

For best results, the statistical interpolation technique (Gandin, 1963) should be used. This requires prior determination of the statistical structure of the variable to be analyzed. Empirical interpolation techniques (Shepard, 1968 and Barnes, 1964) do not require the above statistics. They provide an alternative when the statistical technique is not practical. The method of Jackson et al (1977) requires that the measurement of T_a be coincident in time with the remotely sensed T_s at solar noon.

B.10 A gridded surface inventory and look-up data.

A gridded surface inventory was provided in digital format by Robinson and Associates (1988). Codes and identifications of surface are given in Table 2. Corresponding to each class, a value of surface emissivity and of B coefficient were assigned.

TABLE 1

Surface classification for gridded inventory.

code	predominant surface	B coefficient	emissivity
1	Open	.32	.90
2	Forest	.68	.90
3	Water	1.0	.94
4	Urban	.5	.90
5	Open / forest	.5	.90
6	Open / water	.66	.92
7	Water / forest	.84	.92
8	Water / urban	.41	.90
9	Urban / forest	.75	.92
10	no predominance	.51	.90

This type of classification can be generated from various data sources, including satellite data (Justice et al 1985). It is used in the computation of coefficient B .

B.11 Daily net radiation fields (Rn^{24})

Net radiation is a key product of this method. To obtain an estimate of this field, a relationship was computed from July-August (1985) data for Elora and Toronto reference stations. With regression coefficients of r=.72 for Elora and r=.77 for Toronto, the following relation between the daily net radiation and the 1800 UCT instantaneous (Rn^{i}) net radiation was obtained:

$$R_n^{24}\ (\text{Joules/m}^2) \approx 3\,10^3 + 6\,R_n^{i}\ (\text{Joules/m}^2) \qquad (10)$$

B.12 B term

This field results from the computation of the right term of Equation 1, using grids B7, B9 and B10.

B.13 Daily evapotranspiration

This final result is obtained by combining grids B11 and B12, using Equation 1.

3. VALIDATION AND ERROR ESTIMATES

The following describes tests of an implementation scenario using the residual energy budget technique based on Jackson et al (1977). The scenario required that each of the input fields be properly integrated. Getting the right satellite data was difficult. The following section describes fields generated for July 24, 1985. The Canadian Meteorological Centre weather chart for 1800 UCT on that day showed a low pressure area at the western tip of Lake Superior, with a quasistationnary front extending towards James Bay. The 1800 UCT winds were from the south sector, in the range 15 to 25 km/hour Clouds were present near the frontal region but clear conditions were reported over various locations of the CLI-GRID area.

Changes were made to the scenario to accommodate deficiencies in the data base. Verification of the computed fields were made with real data extracted from the climate archives.

A) Data sets

A.1 Vertical soundings of the atmospheric temperature and water content.

Soundings were obtained for Maniwaki, Quebec (46^{O}23 N, 75^{O}58W). The 1200 UCT and 2400 UCT soundings were linearly interpolated to 1800 UCT for July 24, 1985. The same sounding was used over the whole grid.

A.2 IR to surface temperature conversion table

The LOWTRAN method requires knowledge of satellite sensor response. GOES satellite was used due to the difficulty in obtaining properly navigated 1800 UCT NOAA data. As GOES sensor characteristics could not be obtained, METEOSAT characteristics were used in first approximation. A rural aerosol level and visibility of 20 km were assumed. A correction to the IR brightness temperature was thus computed for the angle of the satellite as function of earth location. Additive correction to an IR temperature of 20^{O}C at 45^{O}N was about +5.2^{O}C at 1800 UCT on July 24, 1985.

A.3 1800 UCT satellite visible and Infrared digital counts.

Figures 3 and 4 show the 1800 UCT images in false colors. The scale at the bottom of each picture allows translation from colour to counts. The IR counts range from one (very warm) to 253 (very cold). The valid VIS counts range from one (dark radiance) to 63 (for a bright radiance). A large portion of the images is cloud free, as shown by the areas with VIS < 23, in blue and light blue, on Figure 4. Typical contrast is evident between water bodies and land on both pictures.

A.4 Cloud mask

Figure 5 shows the cloud mask computed by taking as cloudy all pixels with VIS > 22. Surface observations of cloud opacities at aviation weather sites (Sudbury, North Bay, etc.) were available from the AES digital archives. The opacities in a scale from one to 10 are overlaid on the picture. Opacities above 4 tenths are found over areas classified as cloudy. Cloud opacity of 2 at Wiarton (N44^{O}45', W81^{O}06') is consistent with IR detectable warm cloudiness over southern Lake

Huron and over Georgian Bay. Based on VIS signal, this region is classified as non-cloudy, since cloud over this region is probably thin. However, this particular area is a problem as will be discussed further with field A.9. Future cloud classification for this evapotranspiration algorithm will be based on a combination of VIS and IR thresholds.

A.5 Objective analysis of the precipitable water content (u).

The use of the single Maniwaki sounding (N46^{O}23, W75^{O}58) provided a unique precipitable water content value for the whole grid. This value, 19 mm, might be an overestimate for clear areas since the cloud/no cloud separation was right over Maniwaki.

A.6 Albedo map

Figure 6 shows the albedo map derived from GOES VIS for 1800 UCT on 24 July 1985. False colour representation enhances contrasts between water bodies and land surface. Except over snow or ice, typical albedo values should range from 0.05 to 0.30. All mapped values were below 0.16, with some below 0.05, indicating a possible underestimation. The ratio RF3 (reflected solar radiation) over RF1 (global solar radiation on a horizontal surface) for Toronto Research Station at 1800 UCT was 0.22.

A.7 Midday Surface temperatures estimated from satellite IR

Figure 7 shows the corrected surface temperatures for 1800 UCT. Green areas on the picture were masked by clouds. Over land, there was no routine measurement available to compare the values directly. Hottest spots were estimated in the range from 27^{O}C to 40^{O}C (in yellow). Near the edges of the estimated cloud area (green), there were pixels classified with temperature values below 0^{O}C (light brown). This is due to clouds, undetected using the single VIS threshold classification. The yellow ochre areas were also cooler (T < 15^{O}C) than the remainder of the cloud-free picture.

Over water, there are routine NOAA estimates available for lake water temperature (see Irbe et al, 1982). Maps of July 23, 0800 UCT NOAA estimated water temperatures for lake Erie indicate values from 20^{O}C near the Northern edges of the lake to 22^{O}C over most of the lake and above 23^{O}C in the Southwestern sector and near the Southern edges (see Figure 13, Appendix 1). The ET scheme is not intended to be used over water, but since it automatically evaluates the surface temperatures at every cloud free location, these are available for comparison. The GOES estimate of figure 7 shows values high above 25^{O}C (red and yellow) near the Northern edges of lake Erie, a large central area of temperatures between 16 and 20 ^{O}C (black), and values between 21-22^{O}C (light blue) over the Southwestern portion of the lake. The too high values of the Northern portion of figure 7 are explained by a navigation error of the infrared GOES data that resulted in a shift of the picture to the South. The reader may see that shifting the pattern North by a few pixels would align the GOES image better. Once this shifting is done, a comparison of numerical values indicates that the lake surface temperature using GOES data is underestimated by about two degrees.

Lake Ontario GOES pattern on Figure 7 also requires a shift to the North. Temperatures range then from 10 to 14^{O}C in the Northwest, to 15^{O}C in the centre to 16-20^{O}C near the Southern edge of the lake. Note that these values are extracted from the digital data, since it is difficult to show all these variations in the limited set of colours of Figure 7. Figure 14 shows NOAA lake water temperature estimates for July 23 at 0800 UCT. They range from temperatures < 14^{O}C in a

narrow band over the Northern sector of the lake to about 16°C over the middle to 18°C and above over the Southern sector. Comparison of numerical data indicates that the lake Ontario surface temperatures from GOES data were underestimated by two or three degrees.

A.8 1800 UCT net radiation field

See A.11 below.

A.9 Objective analysis of midday air temperatures (T_a) from reporting stations.

Hourly temperatures over the CLI-GRID area are available from a limited set of 15 Canadian stations. On the other hand, the climatological network provides maximum and minimum data at about 860 climatological stations. The idea is to model the diurnal temperature cycle between the maximum and the minimum temperatures and to extract an hourly temperature estimate. A simple theoretical scheme was used for this purpose. The estimates were objectively analyzed over the CLI-GRID area. Comparison of the values at the location of the 15 hourly stations provided correction parameters which were also objectively analyzed. The original temperature analysis was then corrected. The results of the analysis for 1800 UCT is provided in Figure 8. Most values of this analysis ranged from 18°C to 31°C.

A.10 Gridded surface inventory and look-up data.

Figure 9 shows the classified grid points in colour scales. Lakes (blue), forests (green), open areas (orange) and cities (red) are well delineated. Yellow indicates mixed types 4 to 10 of Table 1.

A.11 Daily net radiation fields (Rn^{24})

Figure 10 shows the daily net radiation field estimated using the 1800 UCT satellite-derived net radiation in equation 10. Highest estimated net radiation (yellow and red) occurs over lakes. Intermediate values (light blue) occur over forests. Lower radiation values, in orange, occur over open areas. Verification data was extracted from the archives for Elora Research Station (43.39N, 80.25W). The ground truth daily value was 14.0 MJ/m^2. The satellite estimate at this location was 20 Mj/m^2. This overestimate might be explained partly due to the presence of clouds during the day in that region.

At the Toronto Meteorological Research Station (43.40N, 79.24W), the ground truth was 15.3 Mj/m^2, but the cloud mask prevented an estimate using satellite data. The daily net radiation estimates in Figure 10 vary from 19 to 25 Mj/day/m^2. Values over the CLI-GRID area rarely exceed 15 Mj/day/m2, which indicates that Figure 10 and therefore equation 10 lead towards an overestimate of the net radiation field.

A.12 B term

Figure 11 shows the computed B (Heat transfer) term in mm/day units. Green areas are masked by clouds. Scale is blue (1 mm/day), orange (2-5 mm/day) and yellow (6 mm/day). Black areas (0 mm/day) cover a large portion of the image and are zero, corresponding to areas of smaller difference between air and surface temperatures. This occurs mostly over forests and lakes. Vertical heat flux occurs over open areas, specially where surface temperature exceeds 25°C (see Figure 7).

A.13 Daily evapotranspiration

The final result of this work is shown on Figure 12 for July 24, 1985. Maximum values appear over water bodies with estimated evaporation of 10 mm/day. Evaporation over water bodies might suffer from errors due to non-negligible heat storage, in addition to the already mentioned error sources. In Figure 12, an intermediate value of 9 mm/day occurs over forest areas. The lowest evapotranspiration values (1 to 8 mm/day) appear over open land. These estimates are within the possible range of ET values (0-14 mm/day). Attempts to verify the final ET estimates will be made in further tests of the improved algorithm.

Table 2 below shows the relative contribution of the net radiation and heat transfer terms to ET at selected locations for the case of July 24, 1985. We already noted in section 2.1 that the heat transfer term would be of smaller magnitude than the net radiation term. The linear correlation coefficient between net radiation and evapotranspiration from the estimates given in Table 2 is r = 0.75. Grid coordinate origin(1,1) is located at Northwest corner of data.

TABLE 2

Relative Contribution of Net Radiation and Heat Flux Terms to ET estimates in mm/day.

Grid coordinates	Surface Type	Net Radiation mm/day	Heat Transfer mm/day	ET mm/day
64, 32	Water	10	0	10
64, 96	Water	10	0	10
80, 45	Water	10	0	10
80, 110	Open	9	-1	8
128, 32	Forest	9	0	9
128, 64	Open	9	0	9
128, 96	Open	8	-2	6
140, 45	Forest	9	0	9
140, 80	Water	8	-1	7
140, 110	Open	8	-1	7
192, 64	Forest	9	0	9
192, 96	Open	8	-4	4
220, 80	Mixed	8	0	8
220, 110	Forest	8	-2	7
240, 110	Forest	8	0	8
245, 115	Mixed	9	-3	6

B) Discussion

The intermediate and final results showed the feasibility of generating multiple location estimates of evapotranspiration, based on satellite data. The comparison of patterns of Figures 5 to 10 with ground truth values indicated where improvements can be made. The significant overestimation of net radiation is an important problem to correct. Another major improvement would be the introduction of NOAA surface temperature estimates.

Further development should incorporate classical treatment of the influence of winds on the B term. Effects and variability of land surface could be subject of a very detailed investigation. Normalized difference index is part of recent ET algorithms and also should be included in the land use parametrization. Finally, the model is not conceptually difficult and its application has been limited mainly due to the effort required in obtaining input data. This last problem will gradually disappear as better data assimilation systems become available.

REFERENCES

Barnes, S.L., 1964: A Technique for Maximizing Details in Numerical Weather Map Analysis. *J. Appl. Meteorol.*, **3**, 396-401.

Benchimol, N., 1985: The Mesoscale Variability of Insolation Over the Lower Fraser Valley Resolved by Geostationary Satellite Data. *Canadian Climate Centre, CCC report* No. 85-8.

Benchimol, N. and J. E. Hay, 1986: An Assessment of the Ability of a Geostationary Satellite-Based Model to Characterize the Mesoscale Variability of Solar Irradiance Over the Lower Fraser Valley. *ATMOSPHERE-OCEAN*, **24**, 128-144.

Bussières, N. and P.Y.T. Louie, 1987: Estimating Regional Evapotranspiration from Satellite Data: A Feasibility Study. *Canadian Climate Centre, CCC report No. 87-12.*

Cooper, D.I., Russo, J.M. and E.M. Perry, 1984: Measurements Uncertainties with Satellite-Derived Surface Temperatures. Pennsylvania State University.

Gandin, L.S. 1963: Objective Analysis of Meteorological Fields. English version published through the *Israel Program for Scientific Translation (IPST)*, Jerusalem, 1965.

Hogg, W. 1986: Production of Gridded Datasets Through Integration and Objective Analysis of Multiple Source Climate Data. CLI-GRID Pilot Project Description. Unpublished *Internal document*, Atmospheric Environment Service, Environment Canada.

Irbe, G.J., Cross, R.K. and A. Saulesleja, 1982: An Operational Program for Monitoring Surface Temperatures of Lakes and Coastal-Zone Waters in Canada from Polar-Orbiting Satellite Infrared Data. *NAFO Sci. Coun. Studies*, **4**, 31-39.

Jackson, R.D., Reginato, R.J., and S.B. Idso, 1977: Wheat Canopy Temperature: A Practical Tool for Evaluating Water Requirements. *Water Resour. Res.* **13**, 651-656.

Justice, C.O., Townshend, J.R.G., Holben, B.N., and C.J. Tucker, 1985: Analysis of the phenology of global vegetation using meteorological satellite data. *Int. J. Remote Sensing*, **6**, 1271-1318.

Kotoda, K., Nakagawa, S., Kai, K., Yoshino, M.M., Takeda, K. and K. Seki, 1985: Application of Equilibrium Evaporation Model to Estimate Evapotranspiration by Remote Sensing Technique. Remote Sensing of Snow and Evapotranspiration, *NASA Conference Publication* **2363**, NASA Goddard Space Flight Center, Greenbelt, Maryland., 115-127.

Monteith, J.L., 1973: *Principles of Environmental Physics* (London: Edward Arnold).

Munn, R.E., 1966: *Descriptive Micrometeorology*, Academic Press, New York, chapter 4.

Nieuwenhuis, G.J.A., Smidt, E.H., and H.A.M. Thunnissen, 1985: Estimation of Regional Evapotranspiration of Arable Crops from Thermal Infrared Images. *Int. J. Remote Sensing*, **6**, 1319-1334.

Price, J.C., 1980: The Potential of Remotely Sensed Thermal Infrared Data to Infer Surface Soil Moisture and Evaporation. *Water Resour. Res.*, **16**, 787-795.

Price, J.C., 1983: Estimating Surface Temperatures from Satellite Thermal Infrared Data - A Simple Formulation for the Atmospheric Effect. *Remote Sens. Environ.* **13**, 353-361.

Rambal, S., Lacaze, B., Mazurek, H. and G. Debussche, 1985: Comparisons of Hydrologically simulated and Remotely Sensed Actual Evapotranspiration from some Mediterranean Vegetation Formations. *Int. J. Remote Sensing*, **6**, 1475-1481.

Reiniger, P. and B. Seguin, 1986: Surface Temperature as an Indicator of Evpotranspiration and Soil Moisture. *Remote Sensing Reviews*, **1**, 277-310.

Seguin, B., and B. Itier, 1983. Using Midday Surface Temperature to Estimate Daily Evaporation from Satellite Thermal IR data. *Int. J. Remote Sensing*, **4**, 371-383.

Serafini, V.V., 1987: Estimation of the evapotranspiration using surface and satellite data. *Int. J. Remote Sensing*, **8**, 1547-1562.

Shepard, D., 1968: A Two-Dimensional Interpolation Function for Irregularly Spaced Data. Proc. 23rd ACM Natl. Conf., Las Vegas, NV, 527-524.

Taconet, O., Bernard, R., and D., Vidal-Madjar, 1986: Evapotranspiration over an Agricultural Region Using a Surface Flux/Temperature Model Based on NOAA-AVHRR Data. *J. Clim. Appl. Meteorol.*, **25**, 284-307.

Tsonis, A.A., 1983: Examination of the Spectral and Spatial Characteristics of the Visible and Infrared GOES Images and applications. Environment Canada, Atmospheric Environment Service, Atmospheric Research Directorate, *Internal Report* No. **ARPB 116 P 39**.

blank page 18

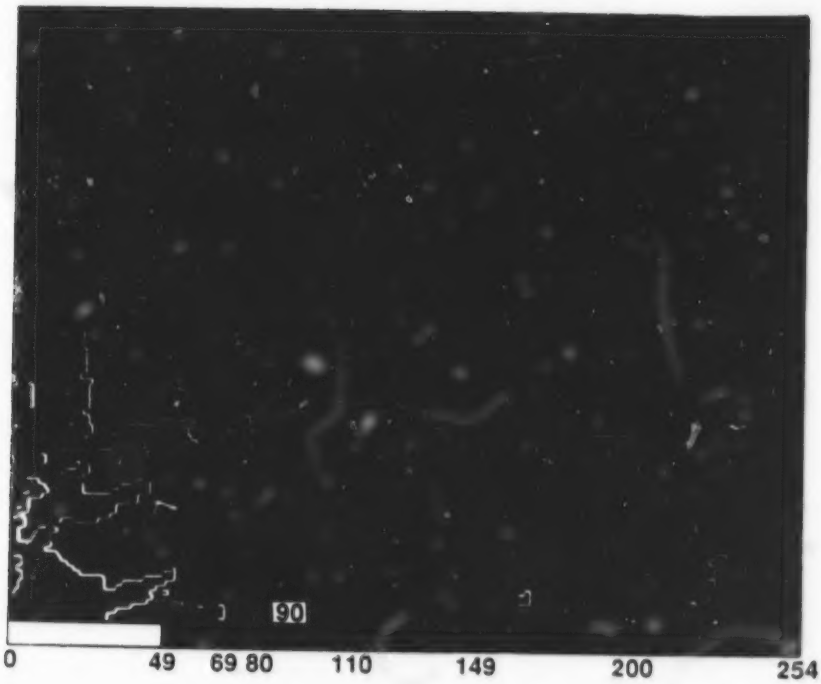

Figure 3 GOES INFRARED on July 24, 1985, at 18Z
(False colour scales)

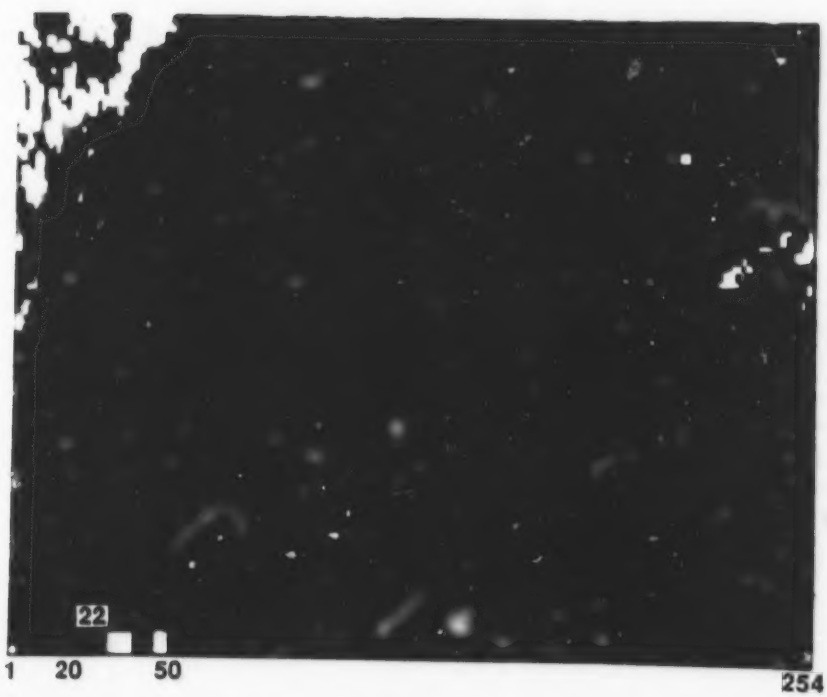

Figure 4 GOES visible picture on July 24, 1985 at 18Z

Figure 5 July 24, 1985, 18Z cloud mask based on level 22 of GOES Vis data. GREEN is cloudy, (Vis>22), BLACK is clear.

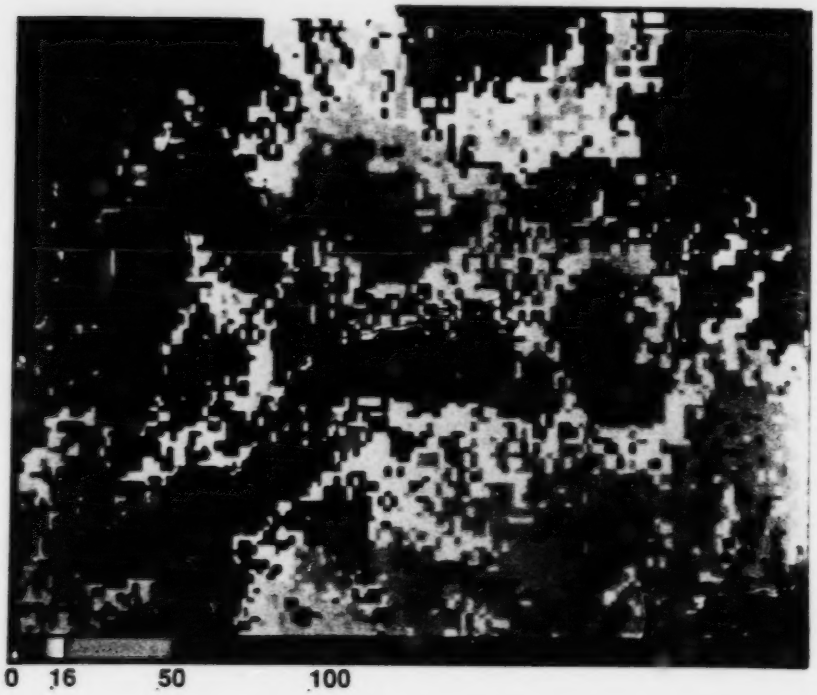

Figure 6 24 July 1985 - 18Z estimated Albedo for GOES view point. No estimate is made over green areas (masked by clouds)

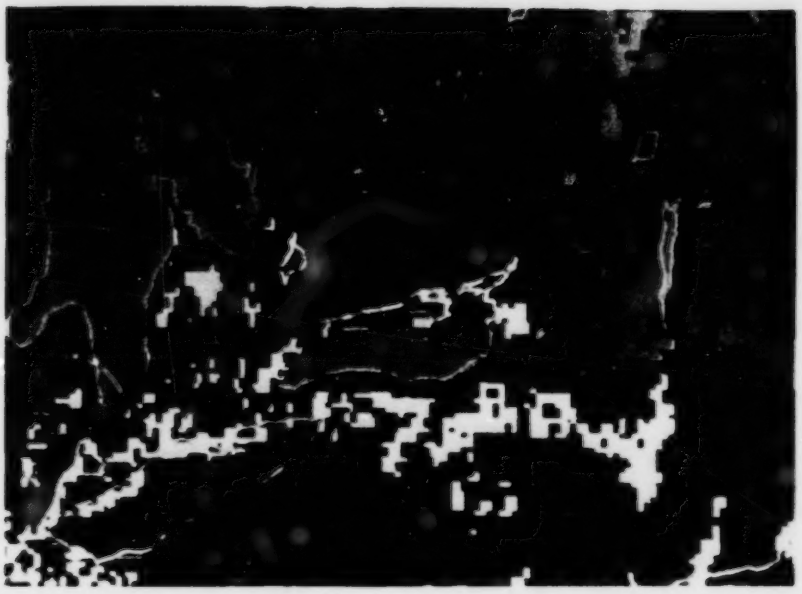

FIGURE 7 SURFACE TEMPERATURE (DEGREES C) ESTIMATED FROM GOES IR CHANNEL FOR JULY 24, 1985, AT 18Z. Colour scale is green (cloud mask), light brown ($<0^{o}$C), yellow ocre (1-15^{o}C), black (16-20^{o}C), light blue (21-22^{o}C), mauve (23-24^{o}C), red (25-26^{o}C), yellow (27-40^{o}C).

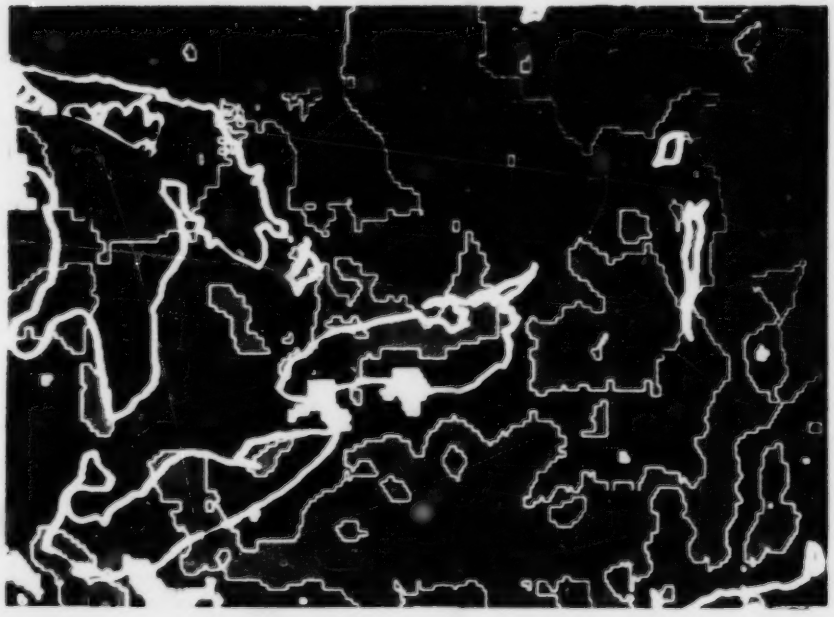

FIGURE 8 AIR TEMPERATURE (OBJECTIVE ANALYSIS OF LAND STATIONS) FOR JULY 24, 1985, AT 18Z. Scale is same as for Figure 7.

FIGURE 9 PREDOMINANT LAND CLASSIFICATION. Water is in blue, agricultural land in orange, forest in green. Urban areas are in red. Yellow indicates mixed types.

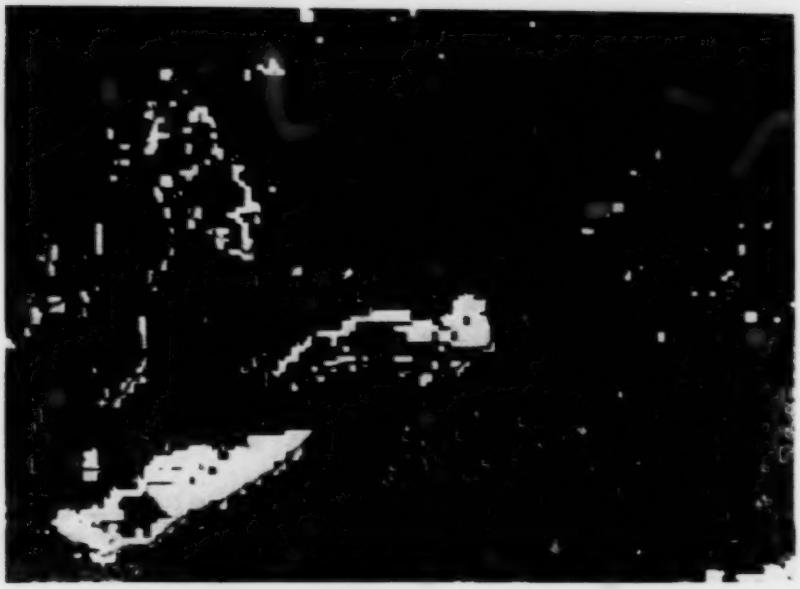

FIGURE 10 24-HOUR NET RADIATION ESTIMATED FROM SATELLITE FOR JULY 24, 1985. Units are megajoules / day / m^2. Scale is: orange (19-20), blue (21-22), yellow (23), red (24-25) and green (cloud mask)

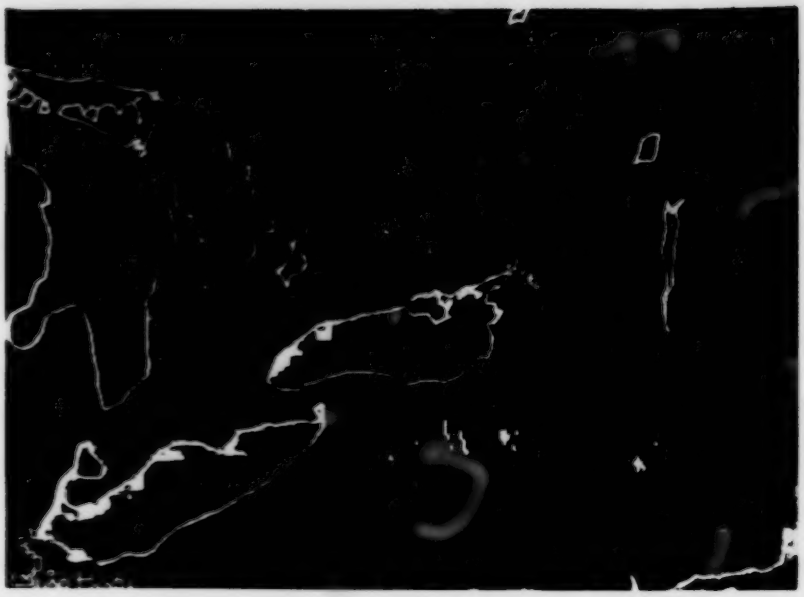

FIGURE 11 HEAT TRANSFER TERM FOR JULY 24, 1985. Units are mm/day. Scale is: black (0), blue (1), orange (2-5), yellow (6) and green (cloud mask).

FIGURE 12 24-HOUR EVAPOTRANSPIRATION ESTIMATED FROM SATELLITE FOR JULY 24, 1985. Units are mm/day. Scale is: black (0), purple (1-6), blue (7-8), orange (9), turquoise (10) and green (cloud mask).

APPENDIX 1. ADDITIONAL INFORMATION

1. The evapotranspiration algorithm was developed during 1987-88 using FORTRAN IV, executable on MODCOMP CLASSIC minicomputers. The source listings amount approximately to 43K (bytes) for the ET main program, 96K for the atmospheric correction module and 68K for the objective analysis module. This software was designed to run with the CLI-GRID system of the Hydrometeorology and Marine Division. At the time of writing of this report, the software is being converted to run on a microcomputer version of CLI-GRID. The source code is being translated in PASCAL. For queries concerning the software, please contact the following address:

HYDROMETEOROLOGY AND MARINE DIVISION (CCAH)
CANADIAN CLIMATE CENTRE
ATMOSPHERIC ENVIRONMENT SERVICE
4905 DUFFERIN STREET
DOWNSVIEW, ONTARIO, M3H 5T4

2. Lake Water temperatures for Lake Erie, Lake Ontario, Lake Huron, Georgian Bay, Lake Superior, Lake Michigan, Bay of Fundy, and other water bodies are routinely analysed pending on the suitability of the NOAA data sets. Figures 13 and 14 were used in data validation (section 3, field A.7). For further information on this product, please contact the Hydrometeorology and Marine Division.

FIGURE 13 SURFACE WATER TEMPERATURE ANALYSIS FOR LAKE ERIE, 08Z, ON JULY , 23 1985. The analysis was based on NOAA satellite data.

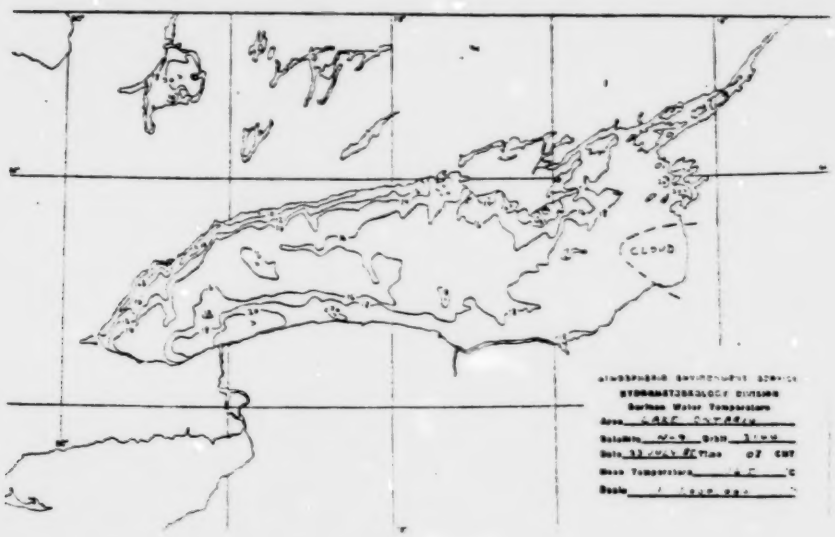

FIGURE 14 SURFACE WATER TEMPERATURE ANALYSIS FOR LAKE ONTARIO, 08Z, ON JULY 23, 1985. The analysis was based on NOAA satellite data.